Journal of Biomedical Optics 6(4), 404–411 (October 2001)

Optical characterization of melanin

Dhiraj K. Sardar
Michael L. Mayo
The University of Texas at San Antonio
Department of Physics and Astronomy
San Antonio, Texas 78249

Randolph D. Glickman
The University of Texas Health Science Center at San Antonio
Department of Ophthalmology
San Antonio, Texas 78229

Abstract. The optical properties of melanin have been characterized for a number of laser wavelengths in the visible region. The index of refraction of melanin is measured by the conventional method of minimum deviation using a hollow quartz prism at these wavelengths. The inverse adding doubling method based on the diffusion approximation and radiative transport theory have been employed to determine the absorption, scattering, and scattering anisotropy coefficients of melanin from the measurements of diffuse transmission, diffuse reflection and collimated transmission using double integrating spheres. The results obtained by the use of inverse adding doubling method have been compared to the Monte Carlo simulation technique. [DOI: 10.1117/1.1411978]

Keywords: lasers; melanin; optical properties; radiative transport.

Paper 20033 received Aug. 3, 2000; revised manuscript received Feb. 20, 2001; accepted for publication Mar. 19, 2001.

1 Introduction

Although there has been a great deal of research on melanin,[1] a systematic and thorough investigation of the optical properties of melanin is lacking. In this paper, we therefore present an in-depth characterization of optical properties of melanin. Melanin is a dark brown pigment abundantly present in human skin and retina, and the coloration of skin depends on the amount of melanin present. The chemical composition of melanin may be distinguished as sulfur-containing (pheomelanin) or sulfur-free (eumelanin), although most physiological melanins are a copolymer of the two types.[1] Typically, hair and skin pigments are characterized as largely pheomelanin with a sulfur content approaching 10%, at least in red hair.[2] In the eye, the cells of the retinal pigment epithelium (RPE) arise from the primitive forebrain, while melanocytes of the uveal tract (iris and choroid) arise from the neural crest.[3] The possibility exists that these two embryologically distinct melanocyte populations synthesize different types of melanin, i.e., eumelanin and pheomelanin; however, studies have found that the melanin in RPE and choroid is similar, with a low sulfur content of about 1% indicating a largely eumelanin composition.[2] In cell culture, iridial melanocytes during the growth phase produce a higher proportion of pheomelanin, while at senescence the melanin composition is predominantly eumelanin.[4] These experimental data suggest that in the mature eye, most of the melanin, at least in the posterior segment, is eumelanin. Nevertheless, the optical properties probably do not differ significantly between eumelanin and pheomelanin.[1]

Melanin strongly absorbs shorter wavelengths of ultraviolet radiation which are very phototoxic to the human eye. It is also believed that melanin-rich skin has natural resistance to skin cancer induced by solar exposure. Since medical applications of coherent radiation from lasers have steadily increased and become more complex, understanding the fundamental optical properties of biological materials is imperative because they influence the distribution and propagation of light in laser-irradiated tissue. Owing to the complex nature of melanin, both absorption and scattering must be considered when evaluating laser propagation through pigmented tissue. Therefore, it is essential to have a thorough knowledge of optical properties of melanin for medical application of lasers. In this regard, we note that the earliest laser medical applications were in ophthalmology and dermatology.[5]

The quantitative distribution of light intensity in biological media can be achieved from the solution of Chandrasekhar's radiative transport equation, Eq. (1).[6] This integro-differential equation describes the rate of change in the intensity of a narrow incident light beam as a function of the optical properties of the medium involved. This is a difficult problem to solve analytically for complex biological media due to their inherent inhomogeneity and irregular shape; nevertheless, by assuming homogeneity and regular geometry of the medium, an estimate of light intensity distribution can be obtained by solving the following radiative transport equation

$$\frac{dI(\mathbf{r},\mathbf{s})}{ds} = -(\mu_a+\mu_s)I(\mathbf{r},\mathbf{s}) + \frac{\mu_a+\mu_s}{4\pi} \times \int_{4\pi} p(\mathbf{s},\mathbf{s}')I(\mathbf{r},\mathbf{s}')d\Omega', \quad (1)$$

where $I(\mathbf{r},\mathbf{s})$ is the intensity per unit solid angle at target location $\mathbf{r}$ in the direction $\mathbf{s}$ ($\mathbf{s}$ is the directional unit vector), μ_a and μ_s are the absorption coefficient and scattering coefficient, respectively, of the medium; $p(\mathbf{s},\mathbf{s}')$ is the phase function, representing scattering contribution from the direction $\mathbf{s}'$ to $\mathbf{s}$, and Ω' is the solid angle.

The first term on the right-hand side of Eq. (1) represents the loss in $I(\mathbf{r},\mathbf{s})$ per unit length in direction $\mathbf{s}$ due to absorption and scattering. The second term denotes the gain in $I(\mathbf{r},\mathbf{s})$ per unit length in direction $\mathbf{s}$ due to scattering from other scattered light $I(\mathbf{r},\mathbf{s}')d\Omega'$ (i.e., light intensity confined in the

Address all correspondence to Dr. Dhiraj K. Sardar. Tel: 210-458-4455; Fax: 210-458-4469; E-mail: dsardar@utsa.edu

1083-3668/2001/$15.00 © 2001 SPIE

elemental solid angle $d\Omega'$) from direction $\mathbf{s}'$. The functional form of the phase function in biological media is usually unknown. In many practical applications, however, the Henyey–Greenstein formula, Eq. (2), provides a good approximation of the phase function, and therefore, is used in all calculations of the inverse adding doubling (IAD) method employed in the present study

$$p(v)=\frac{1}{4\pi}\frac{1-g^2}{(1+g^2-2gv)^{3/2}}, \tag{2}$$

where v is cosine of the angle between $\mathbf{s}$ and $\mathbf{s}'$. The Henyey–Greenstein phase function depends only on the scattering anisotropy coefficient g, which is defined as the mean cosine of the scattering angle, as follows:

$$g=\frac{\int_{4\pi}p(v)v\,d\Omega'}{\int_{4\pi}p(v)d\Omega'}. \tag{3}$$

The value of g ranges from -1 for complete backward scattering to zero for the absolute isotropic scattering to 1 for complete forward scattering.

Although the radiative transport theory gives a more adequate description of the distribution of photon intensity in the turbid medium than does any other model, the general analytical solution is not known yet. Approximate solutions are only available for such restricted conditions as uniform irradiation, or when either absorption or scattering strongly dominates. Although the general solution is not available, an elaborate computational solution is possible using the Monte Carlo (MC) simulation technique.

In order to solve Eq. (1), values for the absorption and scattering coefficients, and scattering phase factor (or anisotropy coefficient), are needed. Therefore, appropriate experimental methods are necessary to measure these optical parameters. As an example, although a single measurement of the total transmission through a sample of known thickness provides an attenuation coefficient for the Lambert–Beer law of exponential decay, it is impossible to separate the attenuation due to absorption from the loss due to scattering. This problem, to some extent, has been resolved by the one-dimensional, two-flux Kubelka–Munk model[7] which has been widely used to determine the absorption and scattering coefficients of biological media,[8–13] provided the scattering is significantly dominant over the absorption. This model provides simple mathematical expressions for determining the optical parameters from the diffuse reflection and transmission measurements. In the past, researchers have applied the diffusion approximation to the transport equation to study biological media.[14–16] Most notably, following the Kubelka–Munk model and diffusion approximation, an excellent experimental method has been described by Van Gemert et al. for determining the absorption and scattering coefficients and scattering anisotropy factor.[17,18]

As mentioned earlier, the diffusion approximation, coupled with the Kubelka–Munk method to determine the tissue optical properties, is valid only when the absorption coefficient is negligibly small compared to the scattering coefficient of the turbid medium under investigation. The absorption coefficient of melanin in the wavelength range of our interest is nonetheless significant and cannot be ignored. Therefore, in our study, the IAD method has been employed to determine both the absorption and scattering coefficients.

In recent years, the IAD method[19] and Monte Carlo simulation technique[20–22] have been shown to provide more accurate estimates of optical properties than any other models previously used. Two dimensionless quantities used in the entire process of IAD are albedo, a, and optical depth, τ, which are defined as follows:

$$a=\mu_s/(\mu_s+\mu_a) \tag{4a}$$

and

$$\tau=t(\mu_s+\mu_a), \tag{4b}$$

where t is the physical thickness of the sample and is measured in cm.

The measured values of the total diffuse reflectance and transmittance, using double integrating spheres, and unscattered collimated transmittance, have been applied to the IAD method to determine the optical properties of the melanin samples. Employing this method, the optical properties are obtained by repeatedly solving the radiative transport Eq. (1) until the solution matches the measured values.

According to Prahl, Van Gemert, and Welch,[19] using only four quadrature points, the IAD method provides optical properties that are accurate to within 2%–3%; higher accuracy, however, can be obtained by using more quadrature points, but it would require increased computation time. They have also stated that the validity of the IAD method for samples with comparable absorption and scattering coefficients is especially important, since other methods based on only diffusion approximation are inadequate. Furthermore, since both anisotropic phase function and Fresnel reflection at boundaries are accurately approximated, the IAD method is well suited to optical measurements for biological materials sandwiched between two glass slides.[19]

2 Materials and Methods

2.1 Melanin Preparation

Melanin was prepared from melanosomes isolated from the bovine retinal pigment epithelium; the details of the preparation of melanosomes were reported by Glickman, Sowell, and Lam.[23] The melanosomes were suspended in 0.25 M sucrose and kept at -20 °C to prevent degradation of the protein layer that encapsulates the melanin granules. After thawing melanosomes were freed from the sucrose solution by centrifugation at 900 rpm for 10 min and decanting the resulting sucrose supernatant. In order to free the internal melanin particles for direct study, the melanosomes were subjected to acid hydrolysis. The melanosome precipitate was suspended in 1 M hydrochloric acid (HCl) and placed in a hot water bath at 60 °C for approximately 8 h to hydrolyze the protein layer. Following the hydrolysis, the sample was again centrifuged through de-ionized water four times to remove any remaining HCl and finally resuspended in 1 ml de-ionized water. After this treatment, the physical appearance of the sample was a brown turbid suspension. Preparation of the sample for optical measurements with the integrating spheres involved fixing a 1-mm-thick O ring with a diameter of 1 inch to a glass slide;

Table 1 The wavelength (λ) dependent indices of refraction (*n*).

Wavelength (nm)	Index of refraction *n*
633	1.28
532	1.29
514	1.29
476	1.30

the O ring acted as a reservoir to retain the melanin sample. The melanin suspension was then transferred with a pipette into the reservoir and a second slide was adhered to the O ring to retain the sample for investigation.

It is important to note that the amount of melanin added to de-ionized water was kept sufficiently low in order to avoid clustering of melanin particles in the final preparation of the sample that was used for particle counting in a calibrated hemocytometer, as well as in the optical measurements. By keeping the number of particles per unit volume low, the possibility of self-screening by the melanin particles during the measurements was minimized.

2.2 Particle Density of Melanin

Because the melanin particles were not actually solubilized by the acid hydrolysis, and remained a particulate suspension, the quantity of melanosomes used in each measurement was referred to as the ''particle density,'' i.e., the number of particles per unit volume. The particle density of melanin in each sample was determined with a Brightline Hemocytometer obtained from Hausser Scientific Co. (Horsham, Pennsylvania) and a Nikon model 66111 microscope (Tokyo, Japan). A small amount of the melanin sample was uniformly distributed on the calibrated surface of the hemocytometer making a thin layer of the sample. The hemocytometer was then placed under the microscope and particle counts were taken from 22 of the 0.05 mm^2 ruled squares on the hemocytometer. The high and low particle counts were discarded, the remaining 20 particle count results were averaged, and the particle count per square millimeter was calculated from which the number per cubic centimeter was derived.

2.3 Measurement of Index of Refraction

The index of refraction of the melanin solution was measured by the method of minimum deviation using a hollow quartz prism. The 60° hollow prism was made of 1 cm×2 cm quartz slides obtained from the NSG Precision Cell, Inc. (Farmingdale, NY). The hollow prism was firmly mounted at the center of an optical spectrometer table. This method was chosen for its simplicity and accuracy. The refractive index of the melanin suspension was determined following published procedures.[24,25] The values of the indices of refraction at different wavelengths are given in Table 1.

2.4 Measurement of Anistropy

Using an independent experimental technique, the anisotropy coefficient g can also be obtained from the measurements of scattered light intensities (I) at various scattering angles (θ) using a goniometer table. The scattering anisotropy coefficient g is given by the average cosine of the scattering angle θ according to Eq. (5)

$$g = \frac{\Sigma_i(\cos\theta_i)I_i}{\Sigma_i I_i}, \tag{5}$$

where the sums are over all values, i, of the scattering angles and intensities.

The scattering anisotropy factor was obtained by irradiating a melanin sample placed at the center of a circular goniometer table with an Oriel model 71400 (Stratford, CT) photomultiplier tube (PMT) mounted at the edge of the table. The PMT was powered by a Bertan model 215 power supply (Hicksville, NY). The sample holder was affixed to the center of the goniometer table. The HeNe laser beam was aligned at a 90° angle with respect to the plane of the glass plates containing the sample, and the PMT was attached to an adjustable pointer which could be rotated around the table for measuring the scattered intensities at different angles as shown in Figure 1. The scattered light intensity was measured between 0° and 180° at an increment of 1° from 0° to 10° of scattering angle,

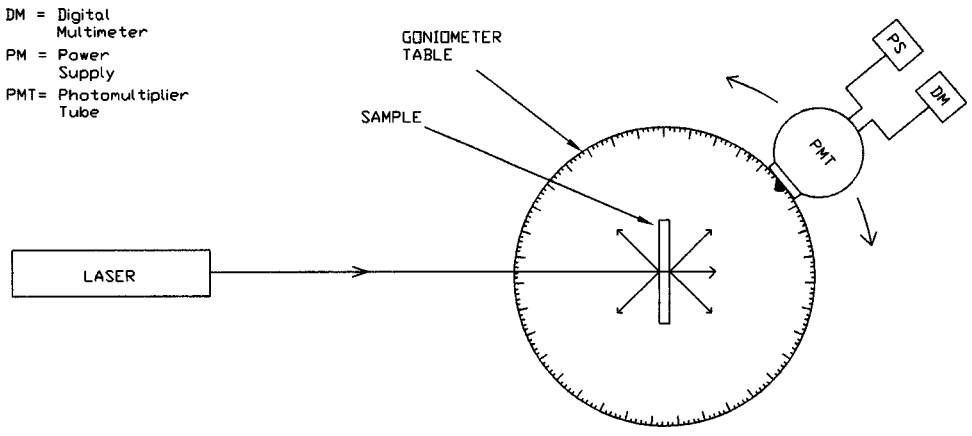

Fig. 1 Schematic of anisotropy measurement.

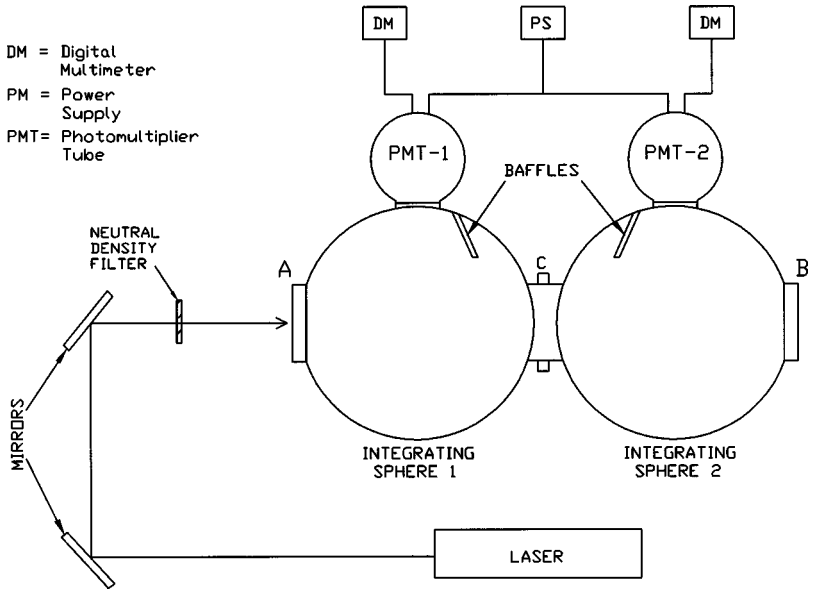

Fig. 2 Schematic of diffuse reflection and transmission measurments.

and an increment of 5° above 10° of scattering angle. Using these values the scattering anistropic factor, *g*, was calculated and found to be 0.94.

2.5 Measurement of Diffuse Reflectance and Transmittance

The total diffuse reflectance and transmittance measurements were taken using double integrating spheres (Oriel model 71400). The prepared sample was placed in a specially designed holder which coupled the two integrating spheres. The sample holder was fabricated at the University of Texas at San Antonio Engineering Machine Shop. The measurements were performed on the melanin sample using the following sources and wavelengths: an argon ion laser for 488 and 514.5 nm, a Nd:yttrium–aluminum–garnet (YAG) for its second harmonic at 532 nm, and a He–Ne laser for 633 nm. The multiline argon ion laser model 2025 from Spectra Physics (Mountain View, CA) was capable of providing wavelengths ranging from 514 to 476 nm, with an average output power of 1–2 W continuous wave (cw). The argon ion laser beam diameter at $1/e^2$ was 1.25 mm and beam divergence was 0.70 mrad at 488 nm. The diode laser-pumped Nd:YAG laser model LCS-DTL-112A from Laser Compact (Moscow, Russia) fitted with a nonlinear frequency doubling crystal provided a second harmonic at 532 nm. The cw output of the laser at 532 nm had a maximum average power of 50 mW. The TEM_{00} laser beam diameter at $1/e^2$ was less than 1.8 mm and beam divergence was about 1.0 mrad. The average output power of the He–Ne laser model 125A from Spectra Physics was 50 mW, the beam diameter at $1/e^2$ was 2 mm, and the beam divergence was 0.70 mrad at 633 nm.

The schematic of the experimental setup employed to measure the total diffuse reflectance and total diffuse transmittance is shown in Figure 2. The intensity of the laser beam was reduced by the use of two Oriel g-66 series, ND=0.82, neutral density filters (Stratford, CT) to prevent the oversaturation of the PMT. The laser was then directed into the entrance port A of integrating sphere 1, whose exit port is coupled with the entrance port of integrating sphere 2; the sample to be studied was mounted at C. The exit port, B, of integrating sphere 2 was covered with a cap with a reflective surface identical to that of the integrating spheres. The diameter of each sphere was 6 in. and each port had a diameter of 1 in. Light leaving the sample was reflected multiple times off the inner surfaces of the spheres. Reflecting baffles within the spheres shielded the PMTs from direct emission from the sample. Port A was equipped with a variable aperture so that the beam diameter could be appropriately controlled. The reflected and transmitted light intensities were detected by two Oriel model 7068 PMTs (Stratford, CT) attached to the two measuring ports. The PMTs were powered by a Bertan, model 215 high voltage power supply (Hicksville, NY). The signals from the PMTs were measured by two Fluke, model 77 series II digital multimeters (Everett, WA). The measured light intensities were then utilized to determine the total diffuse reflectance R_d and total diffuse transmittance T_d by the following expressions:

$$R_d = \frac{X_r - Y}{Z_r - Y}, \tag{6}$$

and

$$T_d = \frac{X_t - Y}{Z_t - Y}, \tag{7}$$

where X_r is the reflected intensity detected by PMT-1 with the sample at C, Z_r is the incident intensity detected with the reflective surface at the exit port of integrating sphere 1, X_t is the transmitted intensity detected by PMT-2 with the sample at C and Z_t is the incident intensity detected by PMT-2 with no sample at C and a reflective surface at B, and Y is the correction factor for stray light measured by PMTs 1 and 2 with no sample at C nor the reflective surface at B. The values of R_d and T_d at different laser wavelengths are given in Table

Table 2 The wavelength (λ) dependent absorption coefficient (μ_a), scattering coefficient (μ_s) and total attenuation coefficient (μ_t), mean free path ($1/\mu_t$), albedo (a), and optical depth (τ) as determined by IAD method using the measured diffuse reflectance (R_d), diffuse transmittance (T_d), and collimated transmittance (T_c).

Experimental				IAD					
Wavelength λ (nm)	R_d	T_d	T_c	a	τ	μ_a (cm^{-1})	μ_s (cm^{-1})	μ_t (cm^{-1})	$1/\mu_t$ (cm)
633	0.353	0.035	0.029	0.995	101.13	5.16	1006.1	1011.3	0.99×10^{-3}
532	0.213	0.031	0.021	0.987	65.06	8.65	642.0	650.7	1.54×10^{-3}
514	0.205	0.035	0.022	0.986	60.21	8.58	593.5	602.1	1.66×10^{-3}
476	0.163	0.021	0.018	0.980	57.85	11.70	566.8	578.5	1.73×10^{-3}

2.

2.6 Collimated Transmittance

The unscattered collimated transmittance T_c was measured to determine the total attenuation coefficient. The collimated laser beam intensities were measured by placing the integrating sphere approximately 2 m from the sample so that the photons scattered off the sample would not be able to enter the small aperture (approximately 3 mm in diameter) at the entrance port of the sphere. The sample was aligned at 90° relative to the incident beam as shown in Figure 3 and measurements were taken.

The collimated transmittance T_c was calculated by the relation

$$T_c=\frac{X_c}{Z_c}, \tag{8}$$

where X_c is the collimated light intensity detected by the PMT-1 with the sample mounted approximately 2 m from the integrating spheres and Z_c is the incident light intensity detected by the PMT-1 with no sample in the light path.

2.7 Inverse Adding Doubling (IAD) Method

In order to solve the radiative transport equation, the IAD algorithm[19] must be supplied with experimentally determined values for the total diffuse reflectance (R_d), total diffuse transmittance (T_d) and collimated transmittance (T_c). The IAD algorithm iteratively chooses values for the dimensionless quantities: albedo a and the optical depth τ and then adjusts the value of the scattering anisotropy g until it matches the experimental values of R_d and T_d. The computed values for the albedo and optical depth are then used to calculate the absorption (μ_a) and scattering (μ_s) coefficients, which are given in Table 2.

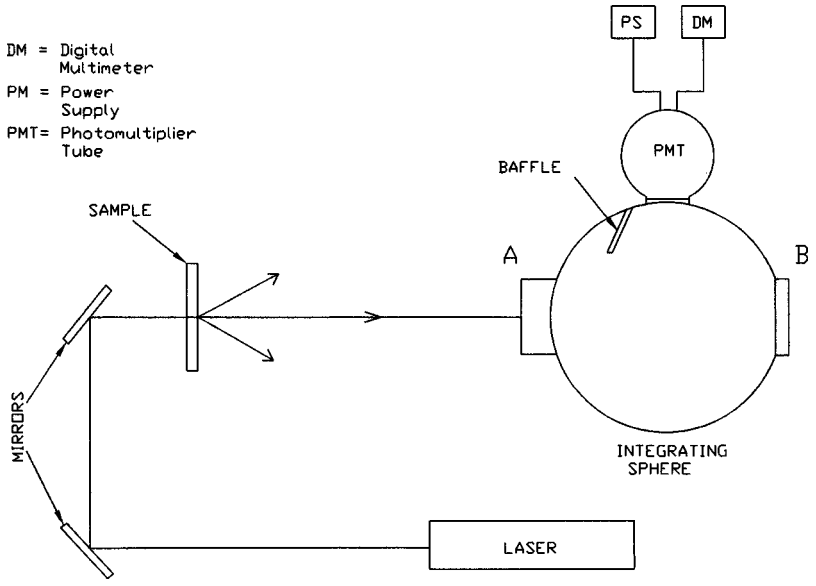

Fig. 3 Schematic of collimated transmission measurement.

Table 3 The wavelength (λ) dependent diffuse reflectance (R_d) and diffuse transmittance (T_d) determined by the experimental and Monte Carlo techniques.

	Experimental		Monte Carlo		Percent difference	
Wavelength λ (nm)	R_d	T_d	R_d	T_d	R_d	T_d
633	0.353	0.035	0.382	0.0381	8.22	7.63
532	0.213	0.031	0.228	0.0.30	7.23	1.31
514	0.205	0.035	0.217	0.037	6.01	5.44
476	0.163	0.021	0.179	0.023	9.32	9.22

2.8 Monte Carlo Simulation

The accuracy of the absorption (μ_a) and scattering (μ_s) coefficients determined by the IAD method was verified by the Monte Carlo (MC) simulation technique. The simulation used the stochastic model to simulate light interaction in biological media. The values for μ_a and μ_s calculated by the IAD method, along with the experimentally determined values for the index of refraction n and scattering anisotropy coefficient g, were used to compute values for R_d and T_d. Fifteen simulations per wavelength were run and the results were averaged. These values were then compared for accuracy with the experimentally determined values for R_d and T_d and found to vary within 10%; these values are given in Table 3. A detailed theoretical description of the MC model in biological media is given by Prahl et al.[26]

3 Results and Discussion

The indices of refraction of melanin in water, measured at 633, 532, 514, and 476 nm, were 1.28, 1.29, 1.29, and 1.30, respectively (see Table 1). Measurements were repeated three times at these wavelengths, and the values agreed to within 4%. The 4% variation in the refractive index values of melanin is likely due to the fact that there was an uncertainty in the measurements of minimum angle of deviation that varied approximately by ±2°. The anistropic scattering factor of melanin was determined to be 0.94 from the goniometric measurement. These measurements were made with a melanin particle density of 4.24×10^5 particles per cubic centimeter.

The total diffuse reflectance and total diffuse transmittance were measured on the melanin samples at 633, 532, 514, and 476 nm. These measurements were repeated three times and the data were in excellent agreement with less than 2% variation. These values along with the measured value of the index of refraction of melanin were input into the IAD program. The output of the IAD program provided two dimensionless quantities: the albedo a and the optical depth τ, defined by Eqs. (4a) and (4b), respectively. The absorption, scattering and anisotropy coefficients were calculated from the values of a and τ. These values are given in Table 2. The absorption coefficients of melanin obtained from the IAD algorithm are plotted as a function of wavelength, and presented in Figure 4. The error bars in this graph spread between 1 and 2.5 cm^{-1}. This

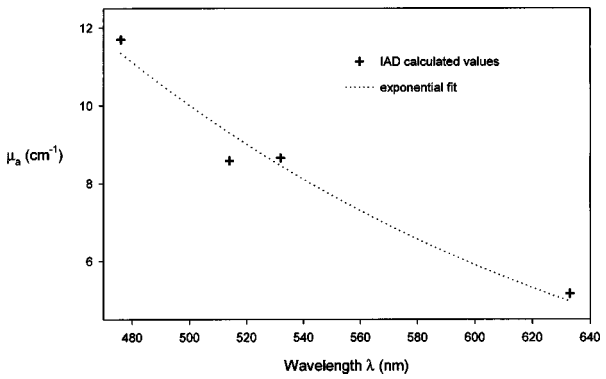

Fig. 4 Absorption coefficient (μ_a) as a function of wavelength.

curve resembles the melanin absorption curve given by Sarna and Sealy.[27] The measured values of diffuse reflectance and transmittance used to calculate the absorption and scattering coefficients of melanin by the IAD methodology were comparable to those generated by the Monte Carlo simulation technique (see Table 3).

The scattering coefficients were found to be much higher than the absorption coefficients of melanin at all wavelengths employed in this study. The scattering coefficient also increased with increasing wavelength, resulting in a larger mean free path (penetration depth) at 633 nm than at 476 nm. Although this was an unexpected finding, we note that the calculated absorption coefficient declined with increasing wavelength in accordance with other studies reported on melanin.[1,28] To the best of our knowledge, there have been no other studies that measured scattering of melanin in isolation. It is possible that the randomized suspension of inhomogeneous melanin particles, produced by the hydrolysis of the melanosome, exhibited a greater degree of scattering than in the intact melanosome where the melanin particles are presumably more orderly arranged within and along the melanoproteins. Nevertheless, the increase of scattering with wavelength is not fully understood at this time, and warrants further investigation.

It is worth comparing the numerical values of the optical parameters, measured here for melanin isolated from bovine RPE melanosomes, to previously published values. There are few, if any, published values for the scattering coefficient, μ_s, of melanin. The values for the absorption coefficient, μ_a, measured in the present study, range from about 5 to 12 cm^{-1}, and are generally lower than values reported for skin or RPE melanin, which have ranged from a high of ~9600 cm^{-1} to a low of ~80 cm^{-1} at mid-visible spectrum wavelengths.[28–30] The large variance in these values may be caused by differences in sample preparation and measurement procedures.[1] In addition, the optical absorption properties of melanin are reported to be affected by the redox state of melanin.[31,32] Many previous studies have estimated melanin absorption either from measurements on intact tissue samples, or measured isolated melanosomes containing their melanoprotein coats, e.g., in the studies of Jacques, Glickman, and Schwartz[28] and Glickman et al.,[33] which reported values for μ_a of intact RPE melanosomes of 2200–2900 cm^{-1} depending on the melanosome fraction. In this study, in order to study the optical properties of melanin alone, the melano-

somes were subjected to acid hydrolysis that stripped them of protein, and caused the remaining melanin to be dispersed in a finely granular suspension. While it is possible that this treatment may have modified the optical properties of melanin, the fact that melanin particles remained an insoluble suspension indicated that the basic polymer structure of the particle retained its integrity, and therefore its optical properties may not have been markedly changed. Finally, some previous studies have relied on measures of bulk optical transmission or reflection to estimate absorption.[34] It is difficult to deconvolve the contribution of scattering from this type of measurement. In the present study, we have measured absorption, scattering, and anisotropy separately. Considered together in the total attenuation coefficient, μ_t, which is the sum of μ_a and μ_s, values in the range of 500–1000 cm^{-1} are obtained, which are comparable to previous estimates of melanin bulk optical absorption.

The actual values for the melanin absorption and scattering coefficients reported in this study have importance for practical applications requiring the prediction of light transport through pigmented tissue, e.g., in the design of treatment models for laser-induced thermotherapy or photodynamic therapy in the eye or in skin, where the degree of pigmentation at the target sites may vary. Variable pigmentation obviously complicates the dosimetry for such treatment modes, because the amount of light delivered will have to be adjusted based on the amount of tissue pigmentation in order to achieve some standard clinical effect. In practice, an estimate of tissue pigmentation could be generated by reflectometry, as has been suggested for skin.[35] This information can be obtained with non- or minimally invasive procedures, and then used together with the optical absorption and scattering parameters of melanin (or other chromophores) to calculate the penetration depth in the target tissue of the relevant light or laser wavelength, and thus to predict the irradiance of the tissue required to achieve a given clinical result. It is hoped that by using this approach, a treatment model can be developed that will reduce the uncertainty in dosimetry that currently is an impediment to the successful implementation of photomedicine.

Acknowledgments

This work was in part supported by the National Science Foundation Grant No. DMR-9616608 and the AFOSR Grant No. F49620-98-1-0210. The Department of Ophthalmology acknowledges the receipt of an unrestricted grant from Research to Prevent Blindness, Inc. The authors would like to thank Scott Prahl (Oregon Medical Laser Center) for the use of the IAD source code and Steven L. Jacques (Oregon Medical Laser Center) and Lihong Wang (Texas A&M University) for the use of the source code for the Monte Carlo model. The source code for both of these programs is available at http://omlc.ogi.edu/software/

References

1. T. Sarna, ''Properties and function of the ocular melanin—a photobiophysical view,'' *J. Photochem. Photobiol., B* **12**, 215–258 (1992).
2. T. P. Dryja,, M. O'Neil-Dryja, and D. M. Albert, ''Elemental analysis of melanins from bovine hair, iris, choroid, and retinal pigment epithelium,'' *Invest. Ophthalmol. Visual Sci.* **18**, 231–236 (1979).
3. J. J. Nordlund, ''The lives of pigment cells,'' *Geriat. Dermatol.* **5**, 91–108 (1989).
4. G. Prota, D. N. Hu, M. R. Vincensi, S. A. McCormick, and A. Napolitano, ''Characterization of melanins in human irides and cultured uveal melanocytes from eyes of different colors,'' *Exp. Eye Res.* **67**, 293–299 (1998).
5. F. A. L'Esperance, Jr., ''Historical aspects of ophthalmic lasers,'' *Ophthalmic Lasers*, 3rd ed., Vol. 1, pp. 13–32, Mosby, St. Louis (1989).
6. S. Chandrasekhar, *Radiative Transfer*, Dover, New York (1960).
7. P. Kubelka, ''New contributions to the optics of intensely light-scattering materials,'' *J. Opt. Soc. Am.* **38**, 448–457 (1948).
8. F. Kottler, ''Turbid media with plane-parallel surfaces,'' *J. Opt. Soc. Am.* **50**, 483–490 (1960).
9. S. Wan, R. R. Anderson, and J. A. Parish, ''Analytical modeling for the optical properties of the skin with in vitro and in vivo applications,'' *Photochem. Photobiol.* **34**, 493–499 (1981).
10. R. R. Anderson and J. J. Parish, ''The optics of human skin,'' *J. Invest. Dermatol.* **77**, 13–19 (1981).
11. S. Ertefai and A. E. Profio, ''Spectral transmittance and contrast in breast diaphanography,'' *Med. Phys.* **12**, 393–400 (1985).
12. M. J. C. van Gemert, R. Verdaasdonk, E. G. Stassen, G. A. C. M. Schets, G. H. M. Gijsbers, and J. J. Bonnier, ''Optical properties of human blood vessel wall and plaque,'' *Lasers Surg. Med.* **5**, 235–237 (1985).
13. M. R. Prince, F. T. Deutsch, R. Margolis, M. M. Mathews-Roth, J. A. Parrish, and A. S. Oseroff, ''Preferential light absorption in atheromas: Implication for laser angioplasty,'' *J. Clin. Invest.* **78**, 295–302 (1978).
14. A. Ishimaru, *Wave Propagation and Scattering in Random Media*, Vol. 1, pp. 202–219, Academic, New York (1978).
15. L. Reynolds, C. C. Johnson, and A. Ishimaru, ''Diffuse reflectance from a finite blood medium: Application to the modeling of fiberoptic catheters,'' *Appl. Opt.* **15**, 2059–2067 (1978).
16. R. A. J. Groenhuis, H. A. Ferwerda, and J. J. Ten Bosch, ''Scattering and absorption of turbid materials determined from reflection measurements. 1: Theory,'' *Appl. Opt.* **22**, 2456–2462 (1983).
17. M. J. C. van Gemert, A. J. Welch, W. M. Star, and M. Motamedi, ''Tissue optics for a slab geometry in diffusion approximation,'' *Lasers Med. Sci.* **2**, 295–302 (1987), and references therein.
18. M. J. C. van Gemert and W. M. Star, ''Relations between the Kubelka-Munk and transport equation models for anisotropic scattering,'' *Lasers Life Sci.* **1**, 287–298 (1987).
19. S. A. Prahl, M. J. C. Van Gemert, and A. J. Welch, ''Determining the optical properties of turbid media by using the inverse adding-doubling method,'' *Appl. Opt.* **32**, 559–568 (1993).
20. J. Hourdakis and A. Perris, ''A Monte Carlo estimation of tissue optical properties for use in laser dosimetry,'' *Phys. Med. Biol.* **40**, 351–364 (1995).
21. M. Hammer, A. Roggan, D. Schweitzer, and G. Muller, ''Optical properties of ocular tissues, an in vitro study using the double-integrating-sphere technique and inverse Monte Carlo simulation,'' *Phys. Med. Biol.* **40**, 963–977 (1995).
22. S. L. Jacques and L. Wang, ''Monte Carlo modeling of light transport in tissues,'' *Optical-Thermal Response of Laser-Irradiated Tissue*, A. J. Welch and M. J. C. van Gemert, Eds., pp. 73–100, Plenum, New York (1995).
23. R. D. Glickman, R. Sowell, and K.-W. Lam, ''Kinetic properties of light-dependent ascorbic acid oxidation by melanin,'' *Free Rad. Biol. Med.* **15**, 453–457 (1993).
24. B. W. Grange, W. H. Stevenson, and R. Viskanta, ''Refractive index of liquid solutions at low temperatures: An accurate measurement,'' *Appl. Opt.* **15**, 858–859 (1976).
25. W. Mahmood bin Mat Yunus, ''Refractive index of dye solutions,'' *Appl. Opt.* **28**, 4268–4269 (1989).
26. S. A. Prahl, M. Keijzer, S. L. Jacques, and A. J. Welch, ''A Monte Carlo model of light propagation in tissue,'' *SPIE Institute Series* **IS5**, 102–111 (1989).
27. T. Sarna and R. C. Sealy, ''Photoinduced oxygen consumption in melanin systems. Action spectra and quantum yields for eumelanin and synthetic melanin,'' *Photochem. Photobiol.* **39**, 69–74 (1984).
28. S. L. Jacques, R. D. Glickman, and J. A. Schwartz, ''Internal absorption coefficient and threshold for pulsed laser disruption of melanosomes isolated from retinal pigment epithelium,'' *Laser-Tissue Interaction VII*, S. L. Jacques, Ed., *Proc. SPIE* **2681**, 468–477 (1996).

29. L. Goldman, ''The skin,'' *Archives of Environmental Health* **18**, 434–436 (1969).
30. S. L. Jacques and D. J. McAuliffe, ''The melanosome: Threshold temperature for explosive vaporization and internal absorption coefficient during pulsed laser irradiation,'' *Photochem. Photobiol.* **53**, 769–775 (1991).
31. T. Sarna, B. Pilas, E. J. Land, and T. G. Truscott, ''Interaction of radicals from water radiolysis with melanin,'' *Biochem. Biophys. Acta.* **833**, 162–167 (1986).
32. W. Korytowski and T. Sarna, ''Bleaching of melanin pigments: Role of copper ions and hydrogen peroxide in auto-oxidation and photo-oxidation of synthetic DOPA-melanin,'' *J. Biol. Chem.* **265**, 12410–12416 (1990).
33. R. D. Glickman, S. L. Jacques, R. T. Hall, and N. Kumar, ''Revisiting the internal absorption coefficient of the retinal pigment epithelium mlanosome,'' *Laser-Tissue Interaction XII: Photochemical, Photothermal, and Photomechanical*, S. L. Jacques, D. D. Duncan, and P. C. Johnson, Eds., *Proc. SPIE* **4257**, 134–141 (2001).
34. N. Kollias and A. Baqer, ''On the assessment of melanin in human skin in vivo,'' *Photochem. Photobiol.* **43**, 49–54 (1986).
35. N. Kollias and A. Baqer, ''Spectroscopic characteristics of human melanin in vivo,'' *J. Invest. Dermatol.* **85**, 38–42 (1985).